HYDROGEN, FUEL CELL & ENERGY STORAGE

Thermodynamic Analysis of a Combined Solar and Geothermal Cycle for Hydrogen and Freshwater Production

Ammar Jalal Abdulrazzaq Al-Tabatabaee | Iraj Mirzaee* | Morteza Khalilian

Mechanical Engineering Department, Engineering Faculty, Urmia University, Urmia, Iran
* Corresponding author, Email: i.mirzaee@urmia.ac.ir

Article Information

Article Type
Research Article

Article History
Received: *01 Aug 2025*
Revised: *29 Sep 2025*
Accepted: *02 Oct 2025*
Published Online: *06 Nov 2025*

Keywords

Multigeneration system
Hydrogen
Freshwater
Solar system

Abstract

This study presents a thermodynamic assessment of a multigeneration system designed to produce power, cooling, heat, hydrogen, and freshwater. The system integrates the Organic Rankine Cycle, a single-effect absorption refrigeration system, a heat pump, a PEM electrolyzer, and a reverse osmosis (RO) unit. It leverages solar energy from two types of solar collectors, geothermal energy, and energy from a PVT (photovoltaic-thermal) collector as its primary energy sources. First, the relevant thermodynamic and thermoeconomic equations for the proposed system are introduced. The entire system is then analyzed using EES (Engineering Equation Solver) software. The system's performance is evaluated, and the impact of various parameters on the effectiveness of the multigeneration system is studied. The examination of exergy destruction in the primary cycles reveals that the evaporator in the ORC cycle experiences the highest exergy destruction rate, at 1526 kW. Furthermore, increasing the collector area and solar radiation of the solar collector results in higher rates of freshwater and hydrogen production. Additionally, an increase in the ORC turbine inlet temperature enhances freshwater and hydrogen production rates, as well as boosts turbine and TEG unit power generation. Finally, the assessment of various working fluids in the ORC cycle demonstrates that n-hexane exhibits the best performance in terms of efficiency and hydrogen and freshwater production rates.

Cite this article: Al-Tabatabaee, A. J. A., Mirzaee, I., Khalilian, M. (2025). Thermodynamic Analysis of a Combined Solar and Geothermal Cycle for Hydrogen and Freshwater Production. DOI: 10.22104/hfe.2025.7165.1321

 Publisher: Iranian Research Organization for Science and Technology (IROST)
DOI: 10.22104/hfe.2025.7165.1321

1 Introduction

Fossil fuels and the process of industrialization have effectively addressed numerous challenges and driven significant progress in society for over two centuries. They have played a pivotal role in enhancing transportation, providing lighting, and contributing to advancements in agriculture, urban development, and overall quality of life. The availability of reliable and powerful energy sources has been key to the rapid expansion of industries, the improvement of transportation systems, and the growth of urban centers, shaping the modern world as we know it today. In 1859, the introduction of commercial fossil oil marked the beginning of a new era in the energy industry. It led to the widespread adoption of internal combustion engines, which became the dominant power source, replacing animals, human labor, turbines, waterwheels, windmills, steam engines, and steam turbines. At the time, the use of commercial fossil oil was viewed as environmentally beneficial, as it replaced whale oil, significantly reducing the demand for whale hunting and the whaling industry, thus having positive effects on whale populations and the environment. As a result, climate change emerged as a significant issue, affecting not only whale populations but the entire planet. The primary sources of greenhouse gas (GHG) emissions are fossil fuels and industrial activities, which contribute to the Earth's atmosphere trapping more heat than is typical, leading to global warming and other environmental challenges.

Energy plays a crucial role in driving the economic advancement of societies and has a profound impact on the environment and human life. It can be broadly categorized into non-renewable sources, such as oil, gas, coal, and wood, and renewable sources, including wind, solar, geothermal, and biogas. Currently, researchers are focusing on developing multigeneration systems powered by renewable energy sources to create more efficient and sustainable energy systems. These systems aim to provide various forms of energy, such as power, heat, and cooling, while minimizing environmental impact and enhancing resource utilization.

In a study by Atiz et al. [1], research was carried out to explore the utilization of integrated geothermal energy from a low-temperature thermal source and evacuated tube solar collectors for electricity generation. The system they proposed showed the best efficiency in terms of power and energy, achieving 6.92% and 21.06% efficiencies, respectively. Kerme et al. [2] examined a multiple energy production system based on a linear parabolic solar collector. Their findings revealed that the solar collector and reverse osmosis water softener were the primary contributors to exergy destruction in the system. In a similar vein, Abdolalipouradl et al. [3] conducted a thermodynamic analysis to compare two novel trigeneration setups that integrated power generation, hydrogen production, and heating, all utilizing geothermal energy. Their study focused on optimizing the performance of these systems in terms of energy efficiency and overall sustainability. Their findings indicated that the exergy efficiency and hydrogen geenration were optimized at a specific temperature of the cogeneration cycle evaporator in the case of the organic Rankine-based system, while the efficiency increased for the Kalina-based cogeneration cycle. In another study, Abdolalipouradl et al. [4] analyzed the thermodynamics of a novel hybrid system utilizing Sablan geothermal wells and the cold energy from liquefied natural gas. They employed a genetic algorithm to optimize the cycle, and the results demonstrated that the net power, thermal efficiency, and exergy were 30,610 kW, 29.16%, and 56.92%, respectively. Hu et al. [5] examined the thermal economic optimization of a geothermal solar hybrid energy system. The research demonstrated that the new method improved electricity generation, lifetime electricity generation, and net present value (NPV) efficiency by 3 to 17 and 14 percent, respectively. Golshanzadeh et al. [6] conducted a comprehensive study on the exergy, energy, and economic and environmental evaluation of a multigeneration system producing electricity and freshwater. This system utilized wind and solar energy as its primary energy sources. The results indicated that increased levels of solar radiation and wind energy significantly influenced the total exergy, work output, and freshwater production of the system. Maali and Khir [7] undertook an examination of the energy and exergy of a hybrid organic Rankine cycle (ORC) power plant integrating both solar and geothermal energy. Their findings identified the steam generator as the primary source of irreversibility in the system, followed by the air-cooled condenser and the turbine. Through the optimization process, the study achieved a 10.35% improvement in exergy efficiency during winter and a 6% enhancement during summer.

Prajapati and Shah [8] undertook a research project focused on generating hydrogen (H_2) using a combination of geothermal and solar power, both of which are key sustainable energy sources. Additionally, the study included a comparative evaluation of various geothermal power plants (GPPs) to assess the output rates and costs associated with hydrogen production.

Kaufmann et al. [9] presented an experimental characterization of a novel fully reversible HTHP/ORC test rig, designed specifically for use in geothermal combined heat and power (CHP) plants. The test rig operates with a 200 kW hot water heating circuit as its heat

source and utilizes a fully reversible 20 kW twin-screw machine that functions as both a compressor and an expander. The HTHP system is capable of handling thermal loads of up to 110 kW, with heat sink outlet temperatures reaching as high as 120 °C, making it an ideal choice for geothermal CHP applications. During the conducted temperature lifts, which ranged from 25K to 57K, coefficients of performance (COP) varied between 6.4 and 3.0. In ORC operation, net electric thermal efficiencies between 5% and 6% were achieved across different heat source mass flow rates and temperatures ranging from 110 °C to 130 °C.

Nazari et al. [10] conducted a comprehensive review of research on the applications of geothermal sources in absorption chillers. This review explored the factors affecting the performance of geothermal absorption chillers, as well as hybrid and polygeneration systems that integrate these chillers. The findings revealed that the efficiency of absorption chillers using geothermal sources is influenced by various factors, such as system configuration, operating conditions, geofluid mass flow rate, and the components used in the system.

Tanbar et al. [11] conducted a thermodynamic and economic assessment of two Organic Rankine Cycle (ORC) systems: the Binary Cycle-Organic Rankine Cycle (BC-ORC) and the Recuperator (BC-ORCR). They utilized low global warming potential (GWP) refrigerants, including R1233zd (E), R1224yd (Z), R1234ze (Z), R1234ze (E), R1243zf, and R1234yf, in conjunction with air- and water-cooled condensers. The findings indicate that the BC-ORCR system employing a water-cooled condenser with R1233zd (E) achieved the highest net output power of 2213 kW and a system efficiency of 10.14%. This system is capable of supporting up to 65% of the electricity demand for the Ulumbu and Ruteng substations.

Bedakhanian et al. [12] conducted an in-depth investigation into the thermodynamic optimization of a geothermal system that integrates a fuel cell unit for energy storage during peak demand periods. This innovative system was designed to concurrently generate cooling, electricity, hydrogen, and freshwater by utilizing an absorption chiller, reverse osmosis, a PEM electrolyzer, and two double Organic Rankine Cycles. The optimal configuration of the proposed geothermal system demonstrated an exergy efficiency of 73.17% and an energy efficiency of 25.25%, while operating at a cost rate of $74.36 per hour. The economic analysis indicated that the ORC1 unit and the PEM electrolyzer represented the highest costs among the system components.

Through an examination of prior research, it is evident that geothermal energy has primarily been utilized as the sole energy source in many earlier studies. In some instances, it has been paired with PTC collectors. Additionally, the implementation of thermoelectric generator (TEG) units in place of the condenser in organic Rankine cycle (ORC) systems remains a topic of significant interest among researchers. Consequently, this study proposes the integration of geothermal energy and photovoltaic-thermal (PVT) solar collectors as the energy sources for the system, while utilizing a TEG unit in lieu of the ORC condenser to generate supplemental power.

2 System Modeling and Description

Figure 1 displays the schematic of the renewable energy system under investigation. This system integrates both solar and geothermal energy sources and is composed of several key components: a heat pump, an organic Rankine cycle (ORC), an absorption refrigeration system, thermal energy storage, a proton exchange membrane (PEM) electrolyzer, and a reverse osmosis (RO) water desalination subsystem. The system's outputs include electricity generation, freshwater production, heating, cooling, and hydrogen generation.

In Figure 1, the schematic illustrates an organic Rankine cycle utilizing isobutane as the working fluid, powered by medium-high temperature geothermal water. The geothermal water exits the production well at point 10, is pumped, and then enters the evaporator of the organic Rankine cycle at point 11. After heat transfer occurs within the ORC, the working fluid moves to Heat Exchanger 1, where it transfers heat before being sent back to the reinjection well. Heat Exchanger 1 is responsible for heating the water used for electrolysis in the system. In the evaporator, the working fluid of the organic Rankine cycle (ORC) is heated before flowing to the turbine at point 16. It exits at point 17, where it releases its heat to the generator of the absorption refrigeration system. A thermoelectric generator (TEG) unit replaces the ORC condenser to generate additional power. Isobutane enters the TEG at point 18, moves to the pump at point 19, where its pressure is increased, and then re-enters the evaporator for further heat absorption. The solar thermal system heats up and stores hot water in thermal energy storage, ensuring that the heat pump can operate continuously, even during periods of low solar radiation. Given that the system is located in a residential area with a consistent demand for heating, cooling, and electricity, continuous operation is essential. The integration of geothermal energy, coupled with a thermal energy storage system, ensures uninterrupted power generation and the provision of cooling, heating, and hot water. The elec-

tricity required for the entire system is supplied by the combined output from the organic Rankine cycle turbine, thermoelectric generator (TEG) unit, and solar photovoltaic-thermal (PV/T) collectors. This electricity not only sustains the operation of the system but also powers the PEM electrolyzer and reverse osmosis (RO) desalination unit, facilitating the production of hydrogen and freshwater to meet the needs of the residential area.

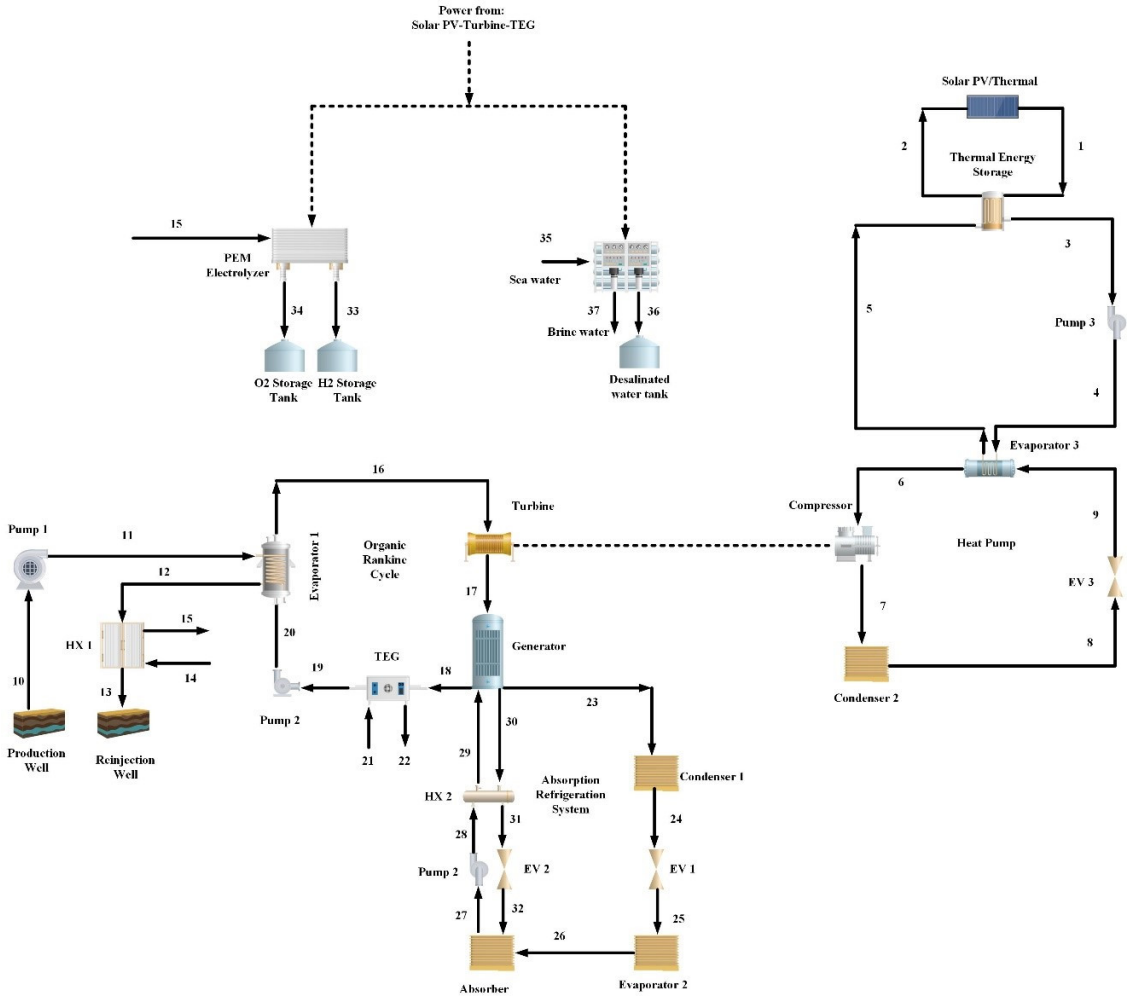

Fig. 1. The diagram of proposed multigeneration system

- The thermodynamic analysis of the system has been conducted by examining mass balance, energy balance, energy and exergy efficiency equations, and exergy loss. The following assumptions have been considered for the analysis: Compressors, Expansion valves, pumps, and turbines operate adiabatically.
- The variations in potential and kinetic energy, along with exergy terms, are considered minimal.
- The processes maintain a steady state and involve steady flow.
- Since there is no chemical reaction between the refrigerant and absorbent, only physical exergy is considered, while chemical exergy is excluded.

$$\sum \dot{m}_{\text{in}} - \sum \dot{m}_{\text{out}} = \frac{dm_{\text{cv}}}{dt}\,, \tag{1}$$

$$\dot{Q} - \dot{W} + \sum_{\text{in}} \dot{m}_{\text{in}}\left(h_{\text{in}} + \frac{V_{\text{in}}^2}{2} + gZ_{\text{in}}\right) - \sum_{\text{out}} \dot{m}_{\text{out}}\left(h_{\text{out}} + \frac{V_{\text{out}}^2}{2} + gZ_{\text{out}}\right) = \frac{dE_{\text{cv}}}{dt}\,, \tag{2}$$

$$\dot{\text{Ex}}_Q + \sum_{\text{in}} \dot{m}_{\text{in}} \text{ex}_{\text{in}} = \sum_{\text{out}} \dot{m}_{\text{out}} \text{ex}_{\text{out}} + \dot{\text{Ex}}_W + \dot{\text{Ex}}_D\,, \tag{3}$$

The energy and exergy balance equations of the proposed multigeneration system can be used to determine the heat and power flow, as well as the exergy loss rates for each piece of equipment, as outlined in Table 1.

Table 1. Energy conservation equations and the rate of exergy loss for each part of the proposed system.

Equipment	Energy balance equations	Exergy destruction rate equations
PV/T collector	$\dot{m}_2 h_2 + \dot{Q}_u = \dot{m}_1 h_1$	$\dot{E}x_{D,\mathrm{PVT}} = \dot{E}x_{\mathrm{sun}} + \dot{E}x_2 - \dot{E}x_1$
TES	$\dot{Q}_{\mathrm{TES}} = U(T_1 - T_0)$	$\dot{E}x_{d,\mathrm{TES}} = \dot{E}x_1 - \dot{E}x_2 - \dot{E}x_Q$
Compressor	$\dot{W}_{\mathrm{comp}} = \dot{m}_6(h_7 - h_6)$	$\dot{E}x_{D,\mathrm{comp}} = \dot{W}_{\mathrm{comp}} + \dot{E}x_6 - \dot{E}x_7$
Condenser 2	$\dot{Q}_C = \dot{m}_7(h_7 - h_8)$	$\dot{E}x_{d,C} = \dot{E}x_7 - \dot{E}x_8$
Pump 1	$\dot{W}_{p1} = \dot{m}_{10}(h_{11} - h_{10})$	$\dot{E}x_{D,p1} = \dot{W}_{p1} - \dot{E}x_{10} + \dot{E}x_{11}$
Pump 2	$\dot{W}_{p2} = \dot{m}_{19}(h_{20} - h_{19})$	$\dot{E}x_{D,p2} = \dot{W}_{p2} - \dot{E}x_{19} + \dot{E}x_{20}$
Pump 3	$\dot{W}_{p3} = \dot{m}_{27}(h_{28} - h_{27})$	$\dot{E}x_{D,p3} = \dot{W}_{p3} - \dot{E}x_{27} + \dot{E}x_{28}$
Pump 4	$\dot{W}_{p4} = \dot{m}_3(h_4 - h_3)$	$\dot{E}x_{D,p4} = \dot{W}_{p4} - \dot{E}x_3 + \dot{E}x_4$
HX1	$\dot{Q}_{\mathrm{HX1}} = \dot{m}_{12}(h_{12} - h_{13}) = \dot{m}_{15}(h_{15} - h_{14})$	$\dot{E}x_{D,\mathrm{HX1}} = \dot{E}x_{12} + \dot{E}x_{14} - \dot{E}x_{13} - \dot{E}x_{15}$
ORC evaporator	$\dot{Q}_{\mathrm{eva,ORC}} = \dot{m}_{11}(h_{11} - h_{12}) = \dot{m}_{16}(h_{16} - h_{20})$	$\dot{E}x_{D,\mathrm{eva,ORC}} = \dot{E}x_{11} + \dot{E}x_{20} - \dot{E}x_{12} - \dot{E}x_{16}$
ORC turbine	$\dot{W}_{t,\mathrm{ORC}} = \dot{m}_{16}(h_{16} - h_{17})$	$\dot{E}x_{D,t,\mathrm{ORC}} = \dot{E}x_{16} - \dot{W}_{t,\mathrm{ORC}} - \dot{E}x_{17}$
ORC TEG	$\dot{Q}_{\mathrm{TEG,ORC}} = \dot{m}_{18}(h_{18} - h_{19}) = \dot{m}_{21}(h_{22} - h_{21})$	$\dot{E}x_{D,\mathrm{TEG,ORC}} = \dot{E}x_{18} + \dot{E}x_{21} - \dot{E}x_{19} - \dot{E}x_{22}$
ARS Generator	$\dot{Q}_{\mathrm{ARS},G} = \dot{m}_{15}(h_{16} - h_{15})$	$\dot{E}x_{d,\mathrm{ARS},G} = \dot{E}x_{17} + \dot{E}x_{29} - \dot{E}x_{18} - \dot{E}x_{23} - \dot{E}x_{30}$
ARS Condenser	$\dot{Q}_{\mathrm{ARS},C} = \dot{m}_{23}(h_{23} - h_{24})$	$\dot{E}x_{d,\mathrm{ARS},C} = \dot{E}x_{23} - \dot{E}x_{24}$
ARS Evaporator	$\dot{Q}_{\mathrm{ARS,eva}} = \dot{m}_{26}(h_{26} - h_{25})$	$\dot{E}x_{d,\mathrm{ARS,eva}} = \dot{E}x_{25} - \dot{E}x_{26}$
ARS Absorber	$\dot{Q}_{\mathrm{ARS,abs}} = \dot{m}_{26}h_{26} + \dot{m}_{32}h_{33} - \dot{m}_{27}h_{27}$	$\dot{E}x_{d,\mathrm{ARS,abs}} = \dot{E}x_{26} + \dot{E}x_{32} + \dot{E}x_{27}$
ARS HX	$\dot{Q}_{\mathrm{ARS,HX2}} = \dot{m}_{30}(h_{30} - h_{31}) = \dot{m}_{28}(h_{29} - h_{28})$	$\dot{E}x_{d,\mathrm{ARS,HX1}} = \dot{E}x_{28} + \dot{E}x_{30} - \dot{E}x_{29} - \dot{E}x_{31}$
PEM	$\dot{W}_{\mathrm{PEM}} = (\dot{m}_{15}h_{15} - \dot{m}_{33}h_{33} - \dot{m}_{34}h_{34})$	$\dot{E}x_{D,\mathrm{PEM}} = \dot{E}x_{15} + \dot{W}_{\mathrm{PEM}} - \dot{E}x_{33} - \dot{E}x_{34}$
RO	$\dot{W}_{\mathrm{RO}} = (\dot{m}_{35}h_{35} - \dot{m}_{36}h_{36} - \dot{m}_{37}h_{37})$	$\dot{E}x_{D,\mathrm{RO}} = \dot{E}x_{35} - \dot{E}x_{36} - \dot{E}x_{37}$

3 Results and Discussions

The simulation of the multigeneration system requires selecting specific input parameters, which are detailed in Table 2.

To ensure the reliability of the obtained results, a comprehensive verification process is conducted. Verifying two subsystems is sufficient to confirm the accuracy of the proposed multigeneration system. Accordingly, the verification focuses on the ORC cycle and the RO desalination subsystem. The ORC cycle is validated using the studies conducted by Zhao et al. [13] and Tzivanidis et al. [14] under identical operating conditions. Detailed results are presented in Table 3.

Based on the initial simulation data, the proposed system achieves energy and exergy efficiencies of 10.29% and 36.77%, respectively. The ORC turbine and PV/T solar collector generate 1834 kW and 59.06 kW of power, respectively. Incorporating a TEG unit into the ORC cycle adds an additional 111.8 kW of power. The cooling system exhibits energetic and exergetic COPs of 0.54 and 0.22, respectively. Overall, the system is capable of producing 796.8 kg/day of hydrogen and 5.52 kg/s of freshwater. Figure 2 depicts the exergy loss rates across different components of the organic Rankine cycle. The results reveal that the evaporator and turbine exhibit the highest exergy losses within the cycle. Exergy degradation in the evaporators is primarily driven by significant temperature differences between the inlet and outlet flows, while irreversibilities in the heat exchangers are largely influenced by these temperature disparities.

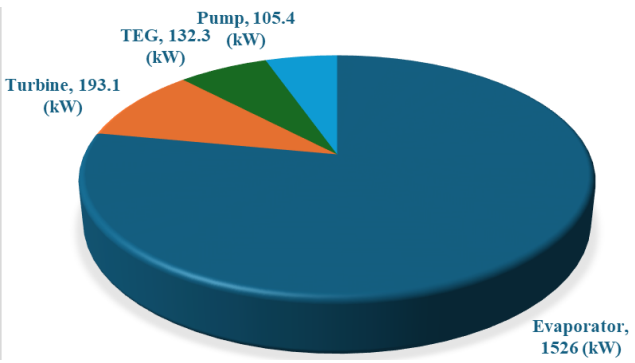

Fig. 2. The rate of exergy destruction varies among the different components of the organic Rankine cycle

Table 2. Input parameters for the modeling of the present study

Parameters	Unit	Value
PV/T		
Dimensions	m	$1.31 \times 2.175 \times 0.18$
Area	m^2	2.85
Cell dimensions	m	0.125×0.125
Maximum temperature	°C	< 134
Sun Temperature	°C	5800
Solar radiation intensity	W/m^2	800
PV/T modules total area	m^2	85
Heat Pump Working fluid: Isobutane		
Inlet temperature of the turbine, T_6	°C	9.5
Outlet temperature of the turbine, T_7	°C	75
Compressor isentropic efficiency	%	85
RO		
Recovery ratio, RR	-	0.3
Number of elements, n_e	-	7
Number of pressure vessels, n_v	-	42
Seawater salinity, X_f	g/kg	43
ORC Working fluid: Isobutane		
Inlet temperature of the turbine,T_{16}	°C	145
Inlet pressure of the turbine, P_{16}	kPa	1500
Isentropic efficiency of Turbine	%	85
Isentropic efficiency of Pump	%	80
Absorption refrigeration system		
Temperature of Evaporator, T_{eva}	°C	5
Temperature of Condenser, T_{con}	°C	40
Temperature of Absorber, T_{abs}	°C	35
Temperature of Generator, T_{des}	°C	100
PEM		
P_{H_2}, P_{O_2}	atm	1
T_{PEM}	°C	80
$E_{\text{act},a}$	kJ/mol	76
$E_{\text{act},c}$	kJ/mol	18
λ_a	-	14
λ_c	-	10
D	mm	50
J_a^{ref}	A/m^2	1.7×10^5
J_c^{ref}	A/m^2	4.6×10^3

Table 3. Thermal efficiency validation results for the present study and references [13, 14].

Working fluid	Present study	Ref [13]	Ref [14]
Pentane	19.49	19.10	19.36
Cyclopentane	22.42	22.36	22.62
Isopentane	18.95	18.91	19.2
Toluene	21.26	21.08	21.35

Figure 3 illustrates the impact of the PVT collector area on the freshwater and hydrogen production rates of the system. The proposed system incorporates three power generation components: the PVT solar collector, the TEG unit, and the ORC cycle turbine. Expanding the PVT solar collector area enhances power generation from the collector, thereby increasing the overall power output of the system. However, it is worth noting that the power contribution of the PVT solar collector is comparatively lower than that of the other two components. A threefold increase in the PVT collector area results in a 3.77% rise in hydrogen production and a 1.85% rise in freshwater production within the system.

Figure 4 displays the impact of changing solar radiation on the PVT collector and its impact on the freshwater and hydrogen production rates. As solar radiation intensifies, the hydrogen production by the PEM electrolyzer increases from 787.4 kg/day to

803.1 kg/day, while the freshwater production by the RO unit rises from 5.493 kg/s to 5.548 kg/s. These improvements are attributed to the enhanced power output of the PVT solar collector under higher solar radiation, which drives greater production efficiency in both subsystems.

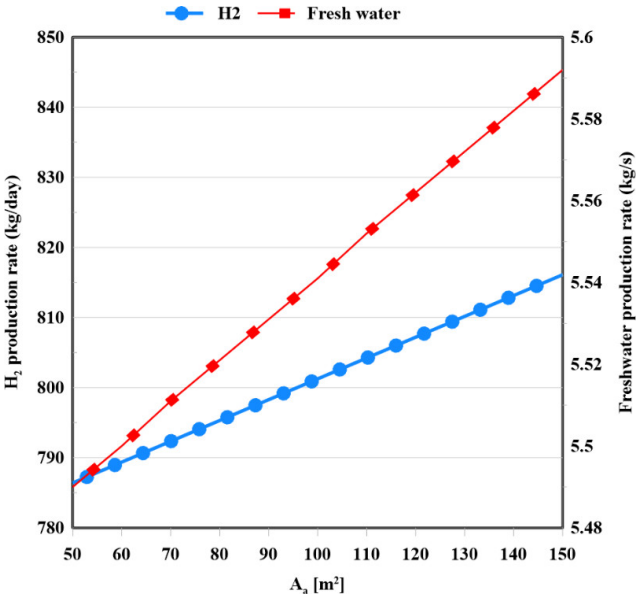

Fig. 3. The influence of the PVT solar collector total area on the amount of hydrogen and freshwater produced by the system

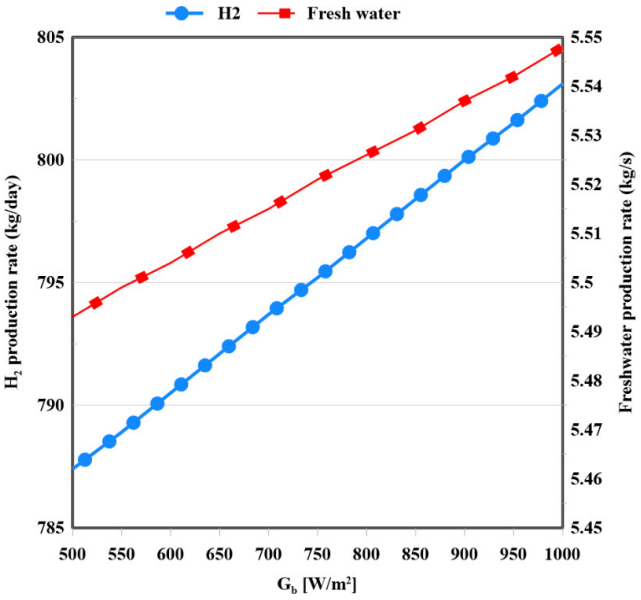

Fig. 4. The influence of PVT solar radiation on the quantity of hydrogen and freshwater produced by the system

Figure 5 illustrates the relationship between the ORC turbine inlet temperature and the power output from both the turbine and the TEG unit. As the turbine inlet temperature increases, the power generated by both components rises. The elevated inlet fluid temperature enhances the turbine's output power and driving force, resulting in an increase in turbine power from 1420 kW to 1817 kW. Similarly, the power produced by the TEG unit grows significantly, rising from 71.5 kW to 393.3 kW.

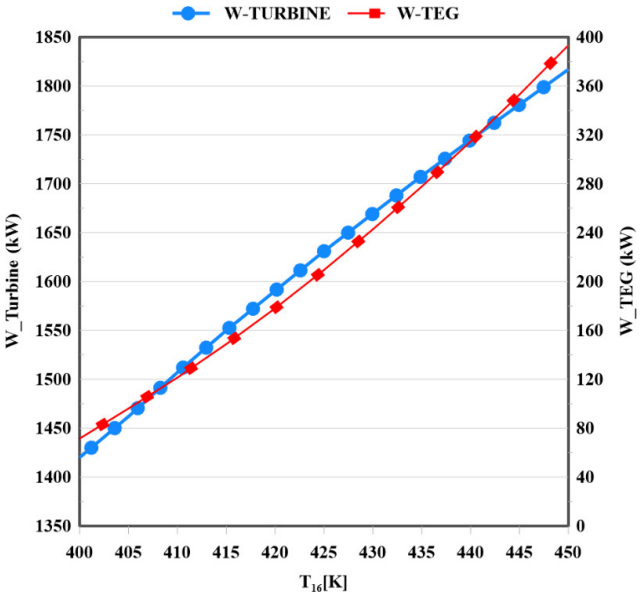

Fig. 5. The power produced by the turbine and TEG influenced by the turbine inlet temperature

Figure 6 illustrates the effect of the ORC turbine inlet temperature on hydrogen production by the PEM electrolyzer and freshwater production by the RO desalination unit. As the turbine inlet temperature increases, both hydrogen and freshwater generation rates show a consistent upward trend. Specifically, as the inlet temperature rises from 400 K to 450 K, the hydrogen production rate increases from 600 kg/day to 909.3 kg/day, while the freshwater production rate grows from 4.82 kg/s to 5.903 kg/s.

The performance of the system with different working fluids in the ORC cycle is illustrated in Figures 7 and 8. Five working fluids – Isobutane, Neopentane, n-Hexane, n-Octane, and R134a – were analyzed for their compatibility with the operating conditions of the ORC cycle. Figures 7 and 8 reveal that n-Hexane achieves the highest energetic and exergetic efficiencies, while R134a exhibits the lowest performance in both metrics. A similar trend is observed in the hydrogen and freshwater generation rates, with n-Hexane producing the highest and R134a the lowest outputs. The superior turbine power generation associated with n-Hexane accounts for these enhanced rates. Thus, it can be concluded that using n-Hexane as the working fluid in the

ORC cycle of the multigeneration system offers optimal performance.

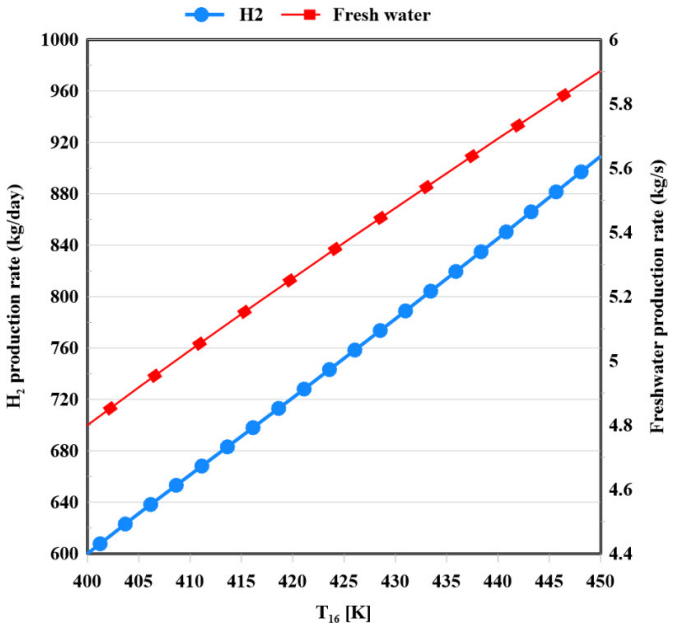

Fig. 6. The influence of turbine inlet temperature on the rate of hydrogen and freshwater production

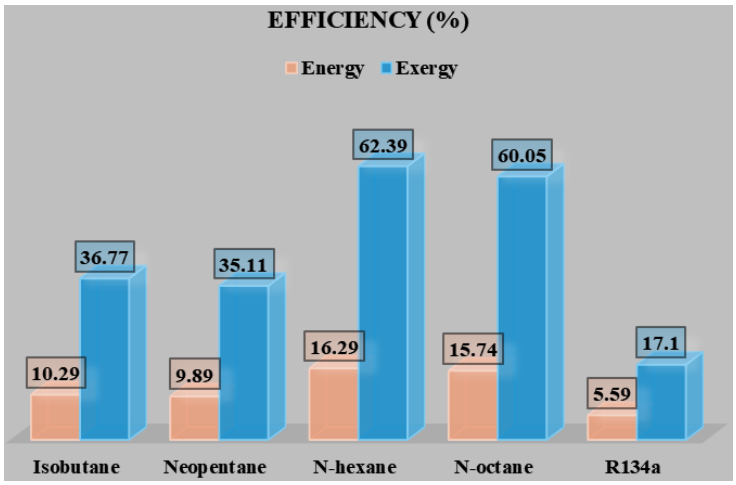

Fig. 7. The influence of various working fluids on the system's energy and exergy efficiency

4 Conclusions

This study presents a thermodynamic analysis of a multigeneration system designed to generate power, heat, cooling, hydrogen, and freshwater. The system under investigation is based on the organic Rankine cycle, a single-effect absorption refrigeration system, a heat pump, a PEM electrolyzer, and a reverse osmosis (RO) unit. It utilizes two distinct solar collectors – geothermal energy and a photovoltaic-thermal (PVT) collector – as its primary energy sources. Initially, the governing equations, along with the thermodynamic and thermoeconomic equations for the proposed system, are presented. The system is then analyzed using EES software. Its performance is evaluated, and the influence of various parameters on the effectiveness of the multigeneration system is investigated. The key find-

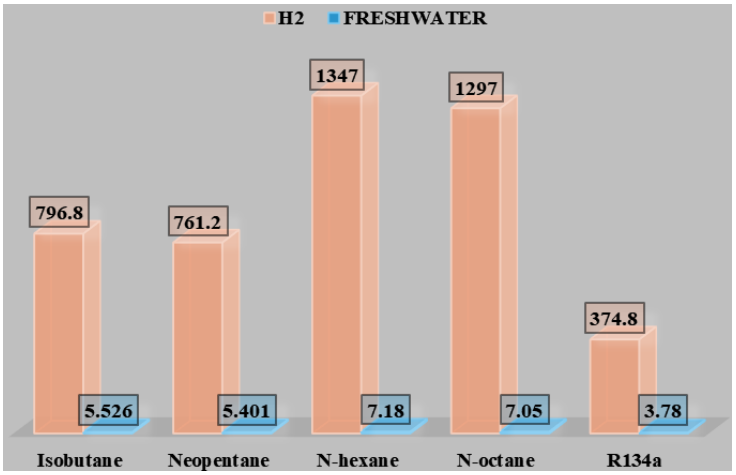

Fig. 8. The influence of various working fluids on the rates of hydrogen and freshwater production

ings from the analysis and simulation of the system are summarized as follows:

- The exergy destruction analysis of the primary cycles shows that in the ORC cycle, the evaporator exhibits the highest exergy destruction rate, at 1526 kW. Increasing the solar collector area leads to higher freshwater and hydrogen production rates in the system.
- Higher solar radiation leads to increased hydrogen and freshwater production rates.

An increase in the ORC turbine inlet temperature leads to higher hydrogen and freshwater generation rates, as well as greater turbine and TEG unit power generation. The evaluation of various working fluids in the ORC cycle shows that n-hexane offers the best performance in terms of efficiency, as well as hydrogen and freshwater production rates.

References

[1] Atiz A. Comparison of three different solar collectors integrated with geothermal source for electricity and hydrogen production. International Journal of Hydrogen Energy. 2020;45(56):31651-66.

[2] Kerme ED, Orfi J, Fung AS, Salilih EM, Khan SUD, Alshehri H, et al. Energetic and exergetic performance analysis of a solar driven power, desalination and cooling poly-generation system. Energy. 2020;196:117150.

[3] Abdolalipouradl M, Rostami M, Khalilarya S, et al. Thermodynamic analysis and comparison of two new tri-generation (hydrogen, power, heating) systems using geothermal energy. Amirkabir Journal of Mechanical Engineering. 2021;53(5):2983-3002.

[4] Abdolalipouradl M, Khalilarya S, Mohammadkhani F, et al. Thermodynamic Analysis of a Novel Power, Cooling, Hydrogen and Oxygen Multi-Generation Combined Cycle Based on the Sabalan Geothermal Wells. Amirkabir Journal of Mechanical Engineering. 2021;53(1):135-54.

[5] Hu S, Yang Z, Li J, Duan Y. Thermo-economic optimization of the hybrid geothermal-solar power system: A data-driven method based on lifetime off-design operation. Energy Conversion and Management. 2021;229:113738.

[6] GolshanZadeh M, Assareh E. Exergy and Energy Analysis of a Multiple Energy Production System Based on Solar and Wind Energy to Produce Clean Electricity and Fresh Water. Journal of Energy Conversion. 2021;7(4):22-36.

[7] Maali R, Khir T. Thermodynamic analysis and optimization of an ORC hybrid geothermal–solar power plant. Euro-Mediterranean Journal for Environmental Integration. 2023;8(2):341-52.

[8] Prajapati M, Shah M. Geothermal-solar hybrid systems for hydrogen production: A systematic review. International Journal of Hydrogen Energy. 2024;67:842-51.

[9] Kaufmann F, von Zabienski J, von Ribbeck L, Ehmann M, Spliethoff H, Schifflechner C. Experimental analysis of a reversible high-temperature heat pump/ORC test rig for geothermal CHP applications. Applied Thermal Engineering. 2025:128360.

[10] Alhuyi-Nazari M, Mukhtar A, Yasir ASHM, Ahmadi MH, Kumar R, Luong T. Applications of

geothermal sources for absorption chillers as efficient and clean cooling technologies for buildings: A comprehensive review. Journal of Building Engineering. 2024;82:108340.

[11] Tanbar F, Febriyanto R, Ariyadi HM, Nugraha AD, Simaremare AA, Supriyanto E, et al. Techno-economic studies of low GWP-organic Rankine cycle for low-level geothermal waste heat utilization in Remote Island of Indonesia. Case Studies in Thermal Engineering. 2025;65:105385.

[12] Bedakhanian A, Assareh E. Exploring an innovative approach to hydrogen generation for fuel cell energy production by integrating a dual organic Rankine system with an absorption chiller powered by geothermal energy. Energy Nexus. 2024;13:100267.

[13] Zhao W, Xie N, Zhang W, Yue J, Wang L, Bu X, et al. Performance characteristics and working fluid selection for high-temperature organic Rankine cycle driven by solar parabolic trough collector. International journal of low-carbon technologies. 2021;16(4):1135-49.

[14] Tzivanidis C, Bellos E, Antonopoulos KA. Energetic and financial investigation of a stand-alone solar-thermal Organic Rankine Cycle power plant. Energy conversion and management. 2016;126:421-33.